Available online at www.sciencedirect.com

ScienceDirect

Procedia CIRP 49 (2016) 14 – 18

www.elsevier.com/locate/procedia

The Second CIRP Conference on Biomanufacturing

Artificial Vascular Bifurcations – Design and Modelling

Xiaoxiao Han[a]*, Richard Bibb[a], Russell Harris[a]

[a]*Loughborough University, Epinal Way, Loughborough, LE11 3TU, UK*

* Corresponding author. Tel.: +44 1509 227567. *E-mail address:* x.han2@lboro.ac.uk

Abstract

Sharp corners in additive manufactured (AM) bifurcated vascular networks cause mechanical aggregation and unrealistic numerical results. A novel parametric bifurcation model was adapted in this paper to generate 3D rounded bifurcations that would solve this problem. Parameters and control variables in the parametric model were selected according to the design rules and the extended parametric map. Preliminary computational fluid dynamic studies were carried out in order to link hydrodynamic risks with local geometry designs. Both positive and negative aspects were found in such designs.

Peer-review under responsibility of the scientific committee of The Second CIRP Conference on Biomanufacturing

Keywords: Bifurcation; Vascular network; CFD; Additive manufacturing; Design.

1. Introduction

Benefiting from the nature of the layer-by-layer method, Additive Manufacturing (AM) is of great interest in medical industries, especially for producing complex grafts and scaffolds in tissue engineering. It enables the manufacture of complex three-dimensional scaffolds or bifurcated vascular networks with controllable geometries. However, an integral element, the design at these complex entities, is a significant bottleneck. Sharp apices at junctions of bifurcated vessels need to be avoided because they are considered risk factors for local mechanical weakness during manufacturing [1]. Increasing the radius of the apex at each bifurcated junction can be one of the solutions. However, artery geometry and corresponding haemodynamic forces have large influences on the vascular pathology development in human circulation [1-6]. A careful design of the arterial bifurcation junction is necessary.

Our previous research [7] presented a novel parametric junction rounding model (Hereinafter referred to as parametric model) of bifurcation vascular networks for tissue engineering. Based on two-and-a-half dimensional surface modelling the model provided an efficient mathematical method that avoids the need for Boolean operations. Furthermore, the data format generated by this method can be transferred into the commonly used STL file format without losing any accuracy.

In this paper, the parametric model is applied to a real application in vertebro-basilar bifurcations. Firstly, the parametric model is described by a flowchart. Real geometry data such as diameters and bifurcation angles are used according to ref [1, 8]. According to design rules adopted from ref [7], control variables will be decided. Because the bifurcation angles exceed the previous parametric map in ref [7], a new $\overline{C}_{\max} - \overline{V}$ relationship is plotted for bifurcation angle 125°, by which, a larger range map is extended. The map governs selections of control variables u_{d1} and u_{d2}. Using the map, parameters and control variables are confirmed which are used to generate 3D models.

Furthermore, in order to discover fluid dynamical factors with the above design, a preliminary CFD study is carried out. CFD models are set up for both sharp and rounded bifurcations. Simulations for a sharp bifurcation ($\phi_{total} = 63^{\circ}$) are validated using existing experimental data. The same boundary conditions are used in a rounded bifurcation

Peer-review under responsibility of the scientific committee of The Second CIRP Conference on Biomanufacturing
doi:10.1016/j.procir.2015.07.021

($\phi_{total} = 85^{\circ}$). Simulations results from both sharp and rounded bifurcation ($\phi_{total} = 85^{\circ}$) are compared. Different fluid behaviours are found and discussed.

Nomenclature

$C_{\max}$ Maximum curvature of a bifurcation junction
$\overline{C}_{\max}$ Non-dimensionalised $C_{\max}$
D_p Parent vessel diameter
D_{d1} Daughter vessel diameter
D_{d2} Daughter vessel diameter
$\overline{D}_{d1}$ Non-dimensionlised D_{d1}
$\overline{D}_{d2}$ Non-dimensionlised D_{d2}
d_p d_{d1} d_{d2} See Figure 4 in ref [7]
$\overline{d}_p$ Non-dimensionlised d_p
$\overline{d}_{d1}$ Non-dimensionlised d_{d1}
$\overline{d}_{d2}$ Non-dimensionlised d_{d2}
u_{d1}, u_{d2} Control variables
V Bifurcation area $\overline{V}$ Non-dimensionlised V

$\alpha = \dfrac{\min(\phi_1,\phi_2)}{\max(\phi_1,\phi_2)}$, $\beta = \dfrac{\overline{D}_{d1}}{\overline{D}_{d2}}$, $\gamma = \dfrac{\overline{d}_{d1}}{\overline{d}_{d2}}$.

ϕ_{total} Bifurcation angle of a vascular branch
ϕ_1, ϕ_2 Bifurcation angle fractions

2. The construction of rounded bifurcations

Detailed construction of rounded bifurcations has been described in previous work [7]. The principle was to sweep Bezier curves to create a semi-tubular bifurcation junction. And then use triangulation filling techniques to efficiently fill two holes in the semi-tubular bifurcation junction. Finally the wall thickness was applied by offsetting the bifurcation surfaces. The design methodology can be found in figure 1.

Fig 1. A summarised design methodology from ref [7].

The model contains more than 10 parameters, all of which affect two main geometry factors: the maximum normalised curvature $\overline{C}_{\max}$ and the normalised volume $\overline{V}$. According to the design rules provided in ref [7], a general bifurcation application consists of five steps as follows:

1. Find the bifurcation angle range
2. Parameter selection according to applications
3. Produce a parametric map
4. Find the controlled variables u_{d1} and u_{d2}
5. Apply the parametric model

2.1. Find the bifurcation angle range

In this paper, this design model is applied in vertebro-basilar bifurcations [1]. According to ref [1], we focus on bifurcation angles: 45°, 85°, 63° and 125°. Both of the inlets diameters are 3.87mm and the outlet diameter is 5mm.

2.2. Parameter selection according to applications

Recalling these normalized parameters in the model [7], we have:

$$\overline{D}_{d1} = \frac{D_{d1}}{D_p},\ \overline{D}_{d2} = \frac{D_{d2}}{D_p},\ \overline{d}_p = \frac{d_p}{D_p},\ \overline{d}_{d1} = \frac{d_{d1}}{D_p},\ \overline{d}_{d2} = \frac{d_{d2}}{D_p} \quad (1)$$

and that

$$\overline{C}_{\max} = \frac{C_{\max}}{\frac{1}{D_p}}, \quad (2)$$

$$\overline{V} = \frac{V}{D_p^3}. \quad (3)$$

Furthermore we have

$$\phi_{total} = \phi_1 + \phi_2, \quad (4)$$

$$\alpha = \frac{\min(\phi_1,\phi_2)}{\max(\phi_1,\phi_2)}, \quad (5)$$

$$\beta = \frac{\overline{D}_{d1}}{\overline{D}_{d2}} \quad (6)$$

And

$$\gamma = \frac{\overline{d}_{d1}}{\overline{d}_{d2}}. \quad (7)$$

According to the current configuration, some parameters are known:

$$D_p = 5\text{mm},\ D_{d1} = 3.87\text{mm},\ D_{d2} = 3.87\text{mm},\ \overline{D}_{d1} = \frac{D_{d1}}{D_p} = 0.774,\ \overline{D}_{d2} = \frac{D_{d2}}{D_p} = 0.774,\ \beta = 1. \quad (8)$$

In order to obtain an appropriate design, four design rules derived from ref [7] are applied in the model. They are:

1. one can use values of $0 \le \alpha \le 1$, u_p =1, $\overline{d}_p$ =2 and $\gamma = \dfrac{1}{\beta}$ for all applications.
2. one should always avoid using small values for both u_{d1} and u_{d2} , less than 0.6 for $\phi_{total} = 85^{\circ}$, for example.
3. one should use $\overline{d}_{d1} + \overline{d}_{d2} = 6$ for all applications.

4. one should use u_{d1} and u_{d2} as the fundamental design variable in order to achieve a targeted maximum curvature while keeping the junction volume within a narrow range.

According to design rule 1 and the normalised parameters we have: $d_p = 10\text{mm}$ and $\gamma = 1$. According to design rule 3 and equation (1) we have: $d_{d1} = 15\text{mm}$ and $d_{d2} = 15\text{mm}$. All cases in the current paper are symmetric bifurcations, and according to equation (5), we have $\alpha = 1$. All parameters for this specific application are finalised and summarised as follows:

$$D_p = 5\text{mm},\ D_{d1} = 3.87\text{mm},\ D_{d2} = 3.87\text{mm}\ \alpha = 1\ \beta = 1\ \gamma = 1$$

$$d_p = 10\text{mm}\ d_{d1} = 15\text{mm}\ d_{d2} = 15\text{mm}. \quad (9)$$

2.3. Reproduce a parametric map

According to the parametric map generated in ref [7], the maximum bifurcation angle is 85°, therefore, we need to reproduce a map using the above parameters and extend the angle range to 125° for the current application.

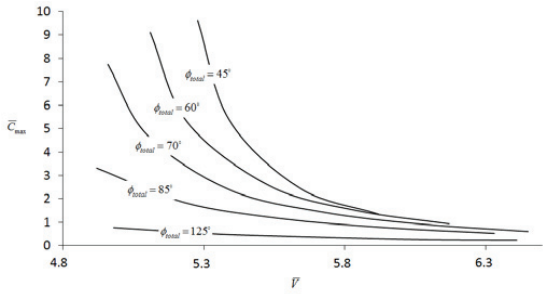

Fig2. Reproduced $\overline{C}_{\max} - \overline{V}$ plots using derived values for different bifurcation angle: $\phi_{total} = 45°$, $\phi_{total} = 60°$, $\phi_{total} = 70°$, $\phi_{total} = 85°$ and $\phi_{total} = 125°$.

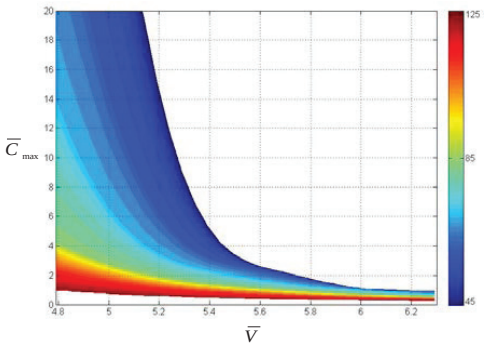

Fig 3. A generalised parametric map in the current application.

Figure 2 illustrates a reproduced $\overline{C}_{\max} - \overline{V}$ using known parameters for different bifurcation angles: $\phi_{total} = 45°$, $\phi_{total} = 60°$, $\phi_{total} = 70°$, $\phi_{total} = 85°$ and $\phi_{total} = 125°$. Figure 3 shows a reproduced map for all bifurcation angles from 45° to 125°.

2.4. Find the controlled variables u_{d1} and u_{d2}

The fundamental control variables in this design are u_{d1} and u_{d2} as α equals to one. High $\overline{C}_{\max}$ will cause stress aggregation during manufacturing while low $\overline{C}_{\max}$, indicating a large $\overline{V}$, will increase blood circulation in the confluence area. In this case we let $\overline{V} = 5.4$ for all bifurcations angles. This gives a $\overline{C}_{\max}$ range which is from 0.44 to 5.37 according to figure 2, which is in a reasonable range. Because $u_{d1} = u_{d2}$ is true for symmetric bifurcation, they can be obtained by back-calculate from the parametric model. All values are shown in table1.

Table1. Value of controlled variables for four cases

ϕ_{total}	$\overline{C}_{\max}$	$\overline{V}$	$u_{d1} = u_{d2}$
125°	0.44	5.4	0.89
85°	1.43	5.4	0.84
63°	3	5.4	0.76
45°	5.37	5.4	0.6

2.5. Apply the parametric model

Both parameters and controlled variables are confirmed using the design rules and the parametric map. 3D bifurcations are then produced which are demonstrate in figure 4. One example from those geometries will be used in the succeeding CFD analysis.

Fig 4. Rounded models for bifurcation angles: 45°, 63°, 85°, and 125°.

3. Computational Fluid Dynamics (CFD) simulations on sharp and rounded bifurcations

Preliminary CFD studies were carried out in order to detect differences of blood/fluid behaviours in a sharp and a rounded bifurcation. Assumptions made to ensure a simple and clear comparison include 1) blood is considered as Newtonian fluid; 2) steady state is simulated; and 3) rectangular tube is used instead for sharp corner bifurcation. The rectangular tube is used because in Ravensbergen [8], hydrodynamic experiments were carried out using rectangular tubes. In their

study, it is indicated that flow phenomena in vertebra-basilar junction models with rectangular model and circular model was the same. They also suggested that rectangular tube has computational and manufactured advantage.

3.1. Governing equation and boundary conditions

A steady state incompressible Navier-Stoke equation written in a primitive variable formulation in terms of the velocity $\mathbf{u}$ and pressure p :

$$-\varepsilon\Delta\mathbf{u}+\mathbf{u}\cdot\nabla\mathbf{u}+\nabla p=\mathbf{f} \quad \text{in } \Omega \tag{10}$$

$$\nabla\cdot\mathbf{u}=0 \quad \text{in } \Omega \tag{11}$$

$$\mathbf{u}=\mathbf{g} \quad \text{on } \Gamma \tag{12}$$

Where ε is viscosity, $\mathbf{f}$ is the body force per unit mass and $\mathbf{g}$ is a given function such that $\int_\Gamma \mathbf{g}\cdot\mathbf{n}d\Gamma=0$, where $\mathbf{n}$ is the unit normal vector to the boundary Γ .

The boundary conditions are described in figure 5.

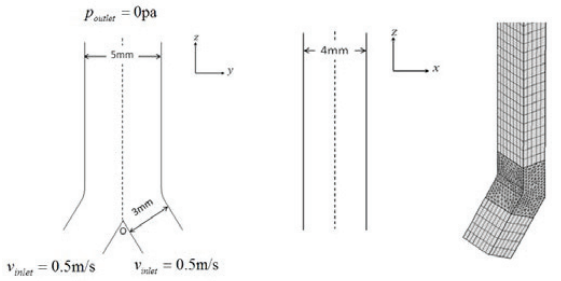

Fig 5. Sharp bifurcation dimensions, boundary conditions and the mesh.

The inlet lengths of each bifurcation are set to be long enough for flow to become fully developed far before the confluent point. At the outlet, the pressure and viscous stress are set to zero. Because all bifurcations in this paper are symmetric, two symmetric planes are used to trim them into symmetries geometries (dashed lines shown in figure 5). Appropriate symmetry boundary conditions are used. The mesh of a bifurcation is shown on the right of figure 5. Very small meshes are used in the area of bifurcation due to complex geometry. Similar meshes are used in the rounded bifurcation.

The calculations were carried out using COMSOL Multiphysics® because of its good adaptation of different design file types. It usually took hours to tens of hours to obtain the results by using fine meshes and running on a 16-core, 32.0GB RAM workstation.

3.2. Sharp corner bifurcation modelling and validation

Using equations (10) – (12) and boundary conditions, results for sharp bifurcation are shown in figure 6.

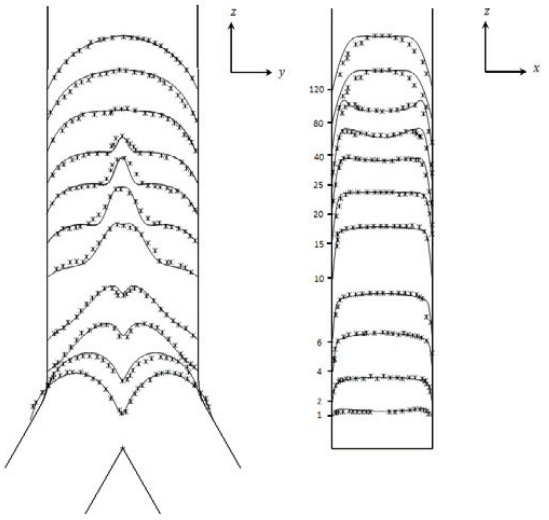

(a) (b)

Fig 6. Simulation results (lines) and experimental data [8] (discrete symbols) comparisons for bifurcation angle 63° in (a) zy plane and (b) zx plane.

Lines shown in figure 6 are velocity results scaled by the mean axial velocity in z different directions while discrete symbols are corresponding experimental data from ref [8]. In figure 6 the simulation results and the experimental results agrees very well, the simulation is, thus, validated. The same simulation governing equations and boundary conditions were adopted in rounded bifurcation with geometries generated from section 2.

3.3. Results and discussions

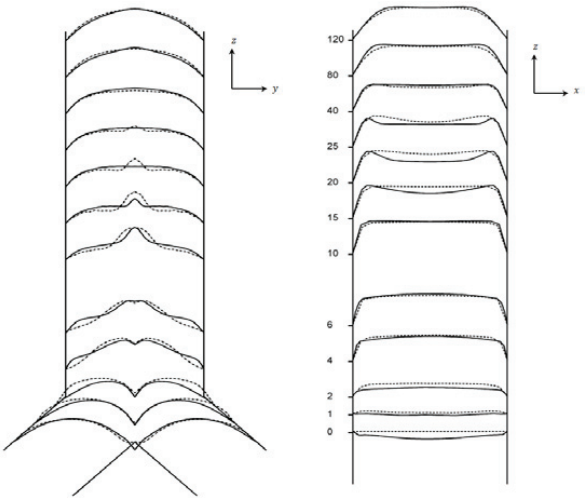

(a) (b)

Figure 7. Comparisons between simulated velocity profiles in sharp bifurcation (interrupted lines) and rounded bifurcation (continuous lines) for bifurcation angle 85° in (a) zy plane and (b) zx plane.

Figure 7 illustrates the simulated velocity profiles for both sharp bifurcation (interrupted lines) and rounded bifurcation (continuous lines) in xz and yz directions. The bottom interrupted lines and continuous lines in figure 7, in xz and yz directions, illustrate velocity profiles at the confluence position for the sharp model, and the same position for the rounded model. Two humps are found in both models. Lower velocity values are found ` model which indicate a larger back flow. Two humps in both models begin to merge downstream and start to generate peaks. Peaks appear after $z = 10$ for both models. However, peaks in the rounded model are narrower compared to the sharp model. Flow becomes flattened further downstream for both designs. The flow profile of a rounded model tends to fully developed quicker than a sharp one as the flow profile peak disappears earlier. At the end of the outlet, both flow profiles are almost coincident.

Back flow in a rounded model is due to flow recirculation appearing in the confluent area, which is shown in figure 8.

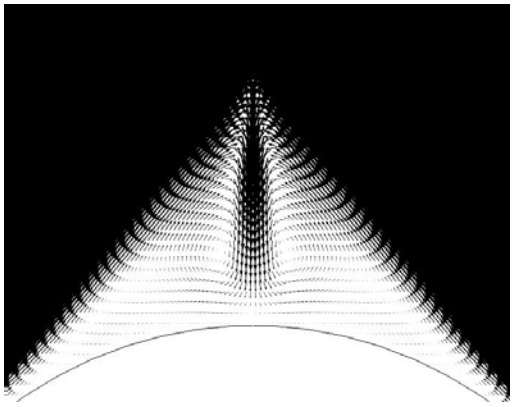

Fig 8. Velocity vectors at the confluence entrance of a rounded bifurcation model.

Firstly, this preliminary CFD study shows that the rounded version of a bifurcation will increase the recirculation risk in the confluence area. Larger confluence areas have a larger recirculation area, thus a lower wall shear stress. Lower wall shear stress is considered an essential factor in the development of cardiovascular diseases. Secondly the rounded model will help in merging two flows quicker thanks to its Bezier Curve Swept design. This can decrease the bifurcation angle effect on flow behaviours. At the last, at the outlet exit, no large differences are discovered for both models. In conclusion, the rounded bifurcation has advantages in avoiding mechanical aggregation and numerical unrealistic results, and merging flows. On the other hand, an increased confluent area has hydrodynamic risks. From this preliminary CFD study, we found that a correlation between wall shear stress and $\overline{C}_{\max} - \overline{V}$ can be observed by analyzing a number of different rounded bifurcations, which is the future work.

4. Conclusion

In this paper, we use the parametric model that was previously generated in the application of a vertebro-basilar artery bifurcation design. Four different bifurcation models were successful generated following the design rules and one extended parametric map. A CFD study was carried preliminarily. Firstly, simulation in a sharp model ($\phi_{total} = 63^{\circ}$) was validated using the hydrodynamic experimental data. Then the same governing equations and boundary conditions are adapted to both a sharp and rounded models with $\phi_{total} = 85^{\circ}$. The comparisons reveal that local geometry of a bifurcation has local effects on flow hydrodynamics. The effects can last downstream. However no obvious influence was found at the outlet exit in this case. Systematic correlations between geometries and hydrodynamics can be obtained once more rounded bifurcations are analyzed.

Acknowledgements

This work is part of the project ArtiVasc3D (http://www.artivasc.eu/). It is financially supported bytheEuropean Union's Seventh Framework Programme (FP/2007-2013) under Grant agreement no.263416 (ArtiVasc3D).

References

[1] Ravensbergen J, Krijger JKB, Verdaasdonk AL, Hillen B, Hoogstraten HW, 1997 The influence of the blunting of the apex on the flow in a Vertebro-Basilar junction model. Journal of Biomechanical Engineering, p. 195-205.
[2] Meng H, Wang Z, Hoi Y, Gao L, Metaxa E, Swartz D, et al., 2007 Complex hemodynamics at the apex of an arterial bifurcation induces vascular remodelling resembling cerebral aneurysm initiation Stroke, p. 1924-31.
[3] Long Q, Xu XY, Bourne M, Griffith TM, 2000 Numerical study of blood flow in an anatomically realistic Aorto-Iliac bifurcation generated from MRI data. Magnetic Resonance in Medicine, p. 565-76.
[4] Kohler U, Marshall I, Robertson MB, Long Q, Xu XY, Hoskins PR, 2001 MRI measurement of wall shear stress vectors in bifurcation models and comparison with CFD predictions. Journal of Magnetic resonance imaging, p. 563-73.
[5] Foutrakis G, Yonas H, Sclabassi R, 1999. Saccular Aneurysm formation in curved and bifurcating arteries. American Journal of Neuroradiology, p. 1309-17.
[6] Marshall I, Zhao S, Papathanasopoulou P, Hoskins P, Xu XY, 2004. MRI and CFD studies of pulsatile flow in healthy and stenosed carotid bifurcation models. Journal of Biomechanics, p. 679-87.
[7] Han X, Bibb R, Harris R., 2015 Design of bifurcation junctions in artificial vascular vessels additively manufactured for skin tissue engineering. Journal of Visual Languages and Computing, p. 238-49.
[8] Ravensbergen J, Krijger J, Hillen B, 1995 Hoogstraten H. Merging flows in an arterial confluence: the vertebra-basilar junction. Journal of Fluid Mechnaics, p. 119-41.